Research Square

Preprints are preliminary reports that have not undergone peer review.
They should not be considered conclusive, used to inform clinical practice,
or referenced by the media as validated information.

Biological Frequency Combs: A Case of Breast Cancer Dynamics

Madhurendra Mishra
University of Delhi
Adarsh Ganesan
adarsh@dubai.bits-pilani.ac.in

Birla Institute of Technology and Science, Pilani - Dubai Campus

Research Article

Keywords: Frequency combs, breast-cancer dynamics, cytotoxic T lymphocytes, CAR-T cells and fractional-order systems

Posted Date: October 30th, 2026

DOI: https://doi.org/10.21203/rs.3.rs-11541345/v1

License: This work is licensed under a Creative Commons Attribution 4.0 International License.
Read Full License

Additional Declarations: The authors declare no competing interests.

BIOLOGICAL FREQUENCY COMBS: A CASE OF BREAST CANCER DYNAMICS

Madhurendra Mishra
Department of Physics
Sri Guru Tegh Bahadur Khalsa College, University of Delhi
New Delhi, India
madhurendramishra24@gmail.com

Adarsh Ganesan
Department of Electrical and Electronics Engineering
BITS Pilani, Dubai Campus
Dubai, United Arab Emirates
adarsh@dubai.bits-pilani.ac.in

ABSTRACT

We explore the emergence of frequency-comb structure in a fractional-order model of breast-cancer dynamics. The model couples tumor cells, cytotoxic T lymphocytes (CTLs), and chimeric antigen receptor (CAR-T) cells through tumor growth, immune activation, saturating cytotoxic killing, cellular decay, and CAR-T-cell therapy. At the nominal parameter values, the three populations undergo relaxation oscillations with a common period, characterized by the frequency comb spectra consisting of frequencies separated by equal intervals. Within the comb regime, the frequency comb spacing increases with the CTL and CAR-T-cell decay rates (d and ζ), the CTL-mediated tumor-cell deactivation rate β, and the CTL-to-CAR-T-cell conversion rate σ. The comb spacing decreases as CTL-dependent CAR-T-cell activation μ, tumor-induced CAR-T-cell deactivation b, or the tumor-cell and CTL carrying capacities (k_1 and k_2) increase. Changes in the tumor-induced CTL deactivation rate ξ and CTL growth rate γ_2 have little effect on the spacing. The comb disappears at sufficiently large β, b, or ζ, while it only appears when μ is increased above a threshold. Ultimately, the comb represents an interesting spectral fingerprint associated with the tumor–immune dynamics.

Keywords Frequency combs · breast-cancer dynamics · cytotoxic T lymphocytes · CAR-T cells · fractional-order systems

1 Introduction

Biological systems are rarely explained by any one reaction in isolation; it is the dynamics of the whole network – feedback, saturation, delay, coupling – that pushes the system toward a fixed state, a periodic orbit, or chaos. This was recognized early on, in the Hodgkin–Huxley model of neuronal excitation [1], in Turing's theory of morphogenesis [2], and in May's simple ecological map [3]. At the cellular level the same logic holds: gene regulation, calcium signaling, circadian rhythms, cell-cycle progression, and immune responses all display bistability, excitability, synchronization, limit cycles, and chaos [4–9], a picture borne out of direct measurements of the p53–Mdm2 [10] and NF-κB [11] pathways and synthetic oscillating gene circuits [12, 13]. Amplitude is not the only carrier of information in these systems – duration, frequency, and phase matter as well [14, 15] – and feedback loops have been shown to select a preferred input frequency [16] and to steer both the amplitude and frequency of competing oscillators [17]. Cancer also displays a similar picture: tumor proliferation, immune recruitment, cytotoxic killing, exhaustion, and treatment continuously feed back on each other, and models of these interactions generate multiple steady states, thresholds, oscillations, and parameter-driven bifurcations [18–21].

A frequency comb is a set of spectral lines that are equally spaced in frequency. The concept originated in nonlinear optical systems through mode locking in high-finesse cavities [22, 23], with major applications in precision metrology and optical clocks. This spectral organization is not restricted only to light. Intrinsic three-wave mixing and three-mode parametric resonance generate phononic frequency combs in micromechanical resonators [24–26]; phononic or mechanical combs have since been observed in graphene, lithium niobate, and overtone resonators [27–30]. Theory has extended the idea to molecular vibrations, twisted van der Waals bilayers, and collective solid-state modes [31–33]. Equally spaced spectral structures have also been reported for coherently generated spin waves [34], ferroelectric polarization dynamics [35], and cosmological evolution [36, 37]. These systems differ greatly in scale and physical origin, but share nonlinear coupling and frequency locking. Biological networks possess comparable ingredients through feedback and modulation. However, the possibility of the recurrent dynamics of a tumor–immune system to produce a frequency comb has not yet been examined.

In this work, we adopt the fractional-order breast-cancer model developed by Ahmed et al. [38] and later extended by Baishya et al. [39]. Its three populations are breast-tumor cells, cytotoxic T lymphocytes (CTLs), and chimeric antigen receptor T cells (CAR-T cells). CTLs and CAR-T cells kill tumor cells through saturating responses; the tumor stimulates CTL proliferation but also deactivates both immune populations. A Caputo derivative represents the dependence of the present tumor–immune response on its prior dynamical history. We calculate the Fourier spectra of all three populations and understand how the model parameters influence the spectra.

2 Dynamical Model

The model presented by Baishya et al. [39] describes tumor growth, the natural immune response, and CAR-T-cell therapy at the population level. Without immune control, the tumor follows logistic growth. Tumor cells induce proliferation of CTLs, and CTLs and CAR-T cells inhibit the tumor by saturating cytotoxic responses. The tumor cells also deactivate CTL and CAR-T cell populations. The resulting system combines growth, activation, killing, saturation, natural decay, and tumor-induced loss. CAR-T cells supply the therapeutic part of the model. In treatment, T lymphocytes are collected from the patient, engineered to recognize tumor-associated antigens, and returned to the body. The modified cells then can activate, multiply and kill malignant cells. We denote the concentrations of tumor cells, CTLs, and CAR-T cells by $u(t)$, $v(t)$, and $w(t)$, respectively, with dynamics governed by

$$ {}^{\mathrm{C}}D_t^{\alpha} u = \gamma_1 u \left(1 - \frac{u}{k_1}\right) - \beta u \left(\frac{v}{l_0 + v}\right) - \rho u \left(\frac{w}{l_1 + w}\right), \tag{1} $$

$$ {}^{\mathrm{C}}D_t^{\alpha} v = \gamma_2 v \left(1 - \frac{v}{k_2}\right) \left(\frac{u}{l_2 + u}\right) - \xi u v - \sigma v \left(\frac{w}{l_3 + w}\right) - d v, \tag{2} $$

$$ {}^{\mathrm{C}}D_t^{\alpha} w = \mu w \left(\frac{v}{l_4 + v}\right) - \zeta w - b u w, \tag{3} $$

with the positive initial conditions

$$ u(t_0) = u_0, \qquad v(t_0) = v_0, \qquad w(t_0) = w_0. \tag{4} $$

All state variables and model parameters take non-negative values.

Equation (1) has one growth term and two loss terms. With no immune cells present, $\gamma_1 u(1 - u/k_1)$ describes logistic growth at intrinsic rate γ_1 and carrying capacity k_1. The term proportional to β accounts for CTL-mediated killing of tumor cells, while the term proportional to ρ accounts for CAR-T-cell-mediated destruction.

The CTL population in equation (2) grows only in the presence of the tumor. Its proliferation factor $u/(l_2 + u)$ increases with tumor concentration before getting saturated, and $1 - v/k_2$ limits the population at the CTL carrying capacity k_2. The CTL population is suppressed by tumor-induced deactivation $-\xi uv$, loss associated with conversion to CAR-T cells $-\sigma vw/(l_3 + w)$, and natural decay $-dv$.

Equation (3) balances CAR-T-cell activation against two loss terms. CTLs activate CAR-T cell population through $\mu wv/(l_4 + v)$ and the response saturates at high CTL concentrations. The natural CAR-T-cell decay is represented by $-\zeta w$, and the contact with tumor cells causes an additional loss $-buw$. The activated CAR-T population then feeds back on the tumor population dynamics through the ρ-dependent term in equation (1).

The model thus presents a coupled dynamics of tumor cell, CTL and CAR-T cell populations. Tumor growth stimulates CTL prolifereation; CTLs kill the tumor and support CAR-T-cell activation; CAR-T cells provide a second cytotoxic pathway; and the tumor population eventually reduces both CTL and CAR-T cell populations. This dynamic process is marked by successive episodes of tumor growth and immune control. Because the resulting cycles are not purely

Table 1: List of parameters and their values.

Parameter	Biological meaning	Nominal value
γ_1	Intrinsic growth rate of tumor cells	0.6387
γ_2	Intrinsic proliferation rate of CTLs	5.7484
β	Inactivation rate of tumor cells by CTLs	0.6
ζ	Decay rate of CAR-T cells	0.4314
ρ	Inactivation rate of tumor cells by CAR-T cells	1.0
k_1	Carrying capacity of tumor cells	1000.0
k_2	Carrying capacity of CTLs	800.0
l_0	Steepness coefficient for CTL-mediated tumor-cell inactivation	20.0
l_1	Steepness coefficient for CAR-T-cell-mediated tumor-cell inactivation	10.0
l_2	Steepness coefficient for tumor-induced CTL proliferation	100.0
l_3	Steepness coefficient associated with CTL-to-CAR-T-cell conversion	20.0
l_4	Steepness coefficient for CTL-mediated CAR-T-cell activation	100.0
ξ	Deactivation rate of CTLs by tumor cells	7.812×10^{-4}
σ	Conversion rate of CTLs to CAR-T cells	0.3
d	Decay rate of CTLs	0.8729
μ	Activation rate of CAR-T cells by CTLs	0.9783
b	Deactivation rate of CAR-T cells by tumor cells	1.0×10^{-4}

sinusoidal, their spectra contain a fundamental frequency and its nonlinear harmonics. We use the term biological frequency comb to represent this ordered array of equidistant frequencies.

The fractional order α introduces memory effects in the dynamics of tumor cell, CTL and CAR-T cell populations. For a differentiable function $f(t)$ and $0 < \alpha < 1$, the Caputo derivative is

$$ {}^{\mathrm{C}}D_t^{\alpha} f(t) = \frac{1}{\Gamma(1-\alpha)} \int_{t_0}^{t} \frac{f'(\tau)}{(t-\tau)^{\alpha}} \, \mathrm{d}\tau, \tag{5} $$

with $\Gamma(\cdot)$ being the Euler gamma function. By writing $\mathbf{x} = (u, v, w)^{\mathsf{T}}$ and ${}^{\mathrm{C}}D_t^{\alpha}\mathbf{x} = \mathbf{F}(\mathbf{x})$, the system can equivalently be recast as the Volterra integral equation

$$ \mathbf{x}(t) = \mathbf{x}(t_0) + \frac{1}{\Gamma(\alpha)} \int_{t_0}^{t} (t-\tau)^{\alpha-1} \mathbf{F}(\mathbf{x}(\tau)) \, \mathrm{d}\tau. \tag{6} $$

Equation (6) models the populations at time t as a cumulative history of growth, activation, cytotoxic killing, and cellular loss. Rather than a biological rate in an ordinary sense, α controls how strongly the earlier tumor–immune trajectories impact the current dynamics. The parameters used in the model and their nominal values are listed in Table 1.

3 Results and Discussion

All the simulations are conducted over a time span $0 \leq t \leq 2000$ with $\Delta t = 0.01$ and $(u_0, v_0, w_0) = (5, 3, 2)$. We used the classical fourth-order Runge–Kutta method for the integer-order system ($\alpha = 1$). However, for $0 < \alpha < 1$, the fractional system was integrated with the Adams–Bashforth–Moulton predictor–corrector scheme applied to equation (6). During each sweep of a parameter, the remaining parameters were held at the nominal values mentioned in Table 1. For computing the Fourier spectra, we discarded the first 200 time units, mean-centered the remaining signal amd applied a Hann window.

When all the parameters are set at their nominal values, the tumor cell, CTL and CAR-T cell populations settle into relaxation oscillations [Figure 1(a)]. Tumor, CTL, and CAR-T-cell responses differ in amplitude and pulse shape, but not in period – all three recur on the same timescale, a fact that stands out far more clearly in the frequency domain producing one dominant fundamental peak and a series of weaker peaks spaced at equal intervals [Figure 1(b)]. This shared harmonic sequence is what we call a biological frequency comb.

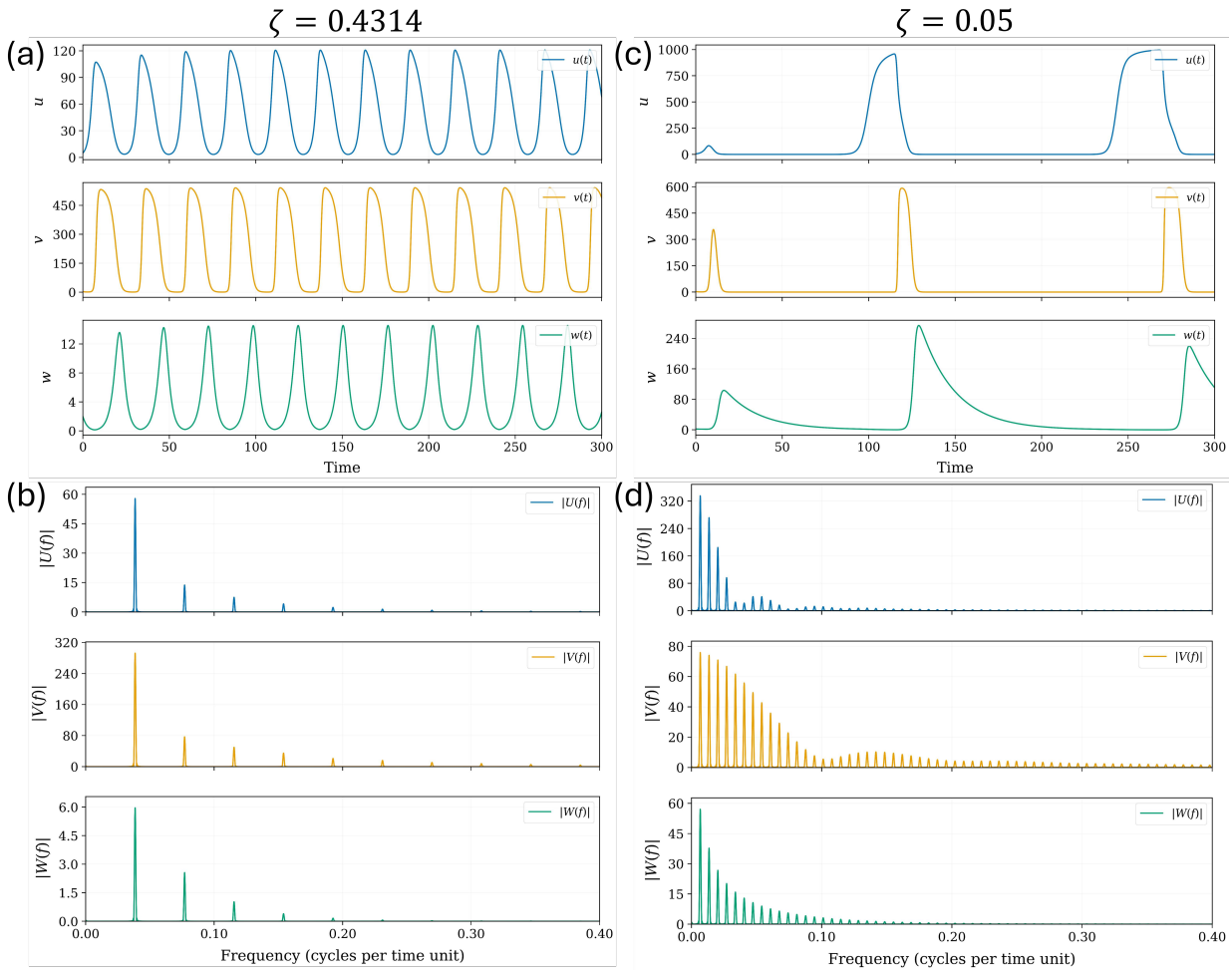


Figure 1: Tumor-cell, CTL, and CAR-T-cell responses in the time domain and their Fourier spectra. Panels (a) and (b) are obtained with the nominal parameter values, while panels (c) and (d) are for $\zeta = 0.05$, keeping all other parameters fixed at their nominal values.

The effect on the recurrence time can be seen by reducing the CAR-T-cell decay rate to $\zeta = 0.05$. All three populations then appear as more widely separated bursts [Figure 1(c)]. CAR-T cells remain in the system for a longer time, and hence both the fundamental frequency and the distance between neighboring lines become smaller. Also, the width of individual bursts are shorter, and hence their spectra produce a larger number of resolved higher harmonics with greater magnitudes [Figure 1(d)].

Figures 2, 3 and 4 show how different parameters influence the frequency comb spacing. Increasing β, the CTL-mediated tumor-cell inactivation rate, moves the combs towards higher frequencies and increases their separation. However, at large-enough values of β, the frequency combs cease to exist. An increase in the CAR-T-mediated inactivation rate ρ initially reduces the frequency comb spacing before the spectrum levels off. While ξ does not influence the frequency comb spacing, the higher harmonics do weaken at higher values of ξ. As b increases, the comb frequencies decrease before getting entirely vanished. σ, in contrast, increases the comb frequencies. While μ decreases the comb frequencies, the frequency comb vanishes at low-enough values of $\mu \lesssim 0.8$.

The effects of cellular decays, carrying capacities, and growth/proliferation rates on the frequency comb dynamics are presented in Figure 3. An increase in both CTL decay rate d and CAR-T-cell decay rate ζ increases the frequency comb spacing. In contrast, the carrying capacities k_1 and k_2 initially decrease the frequency comb spacing before the spectrum levels off. When the tumor growth rate γ_1 is increased above a threshold value, the comb appears and its spacing increase with any further increase in γ_1. However, the proliferation rate of CTLs γ_2 does not change the frequency comb spacing.

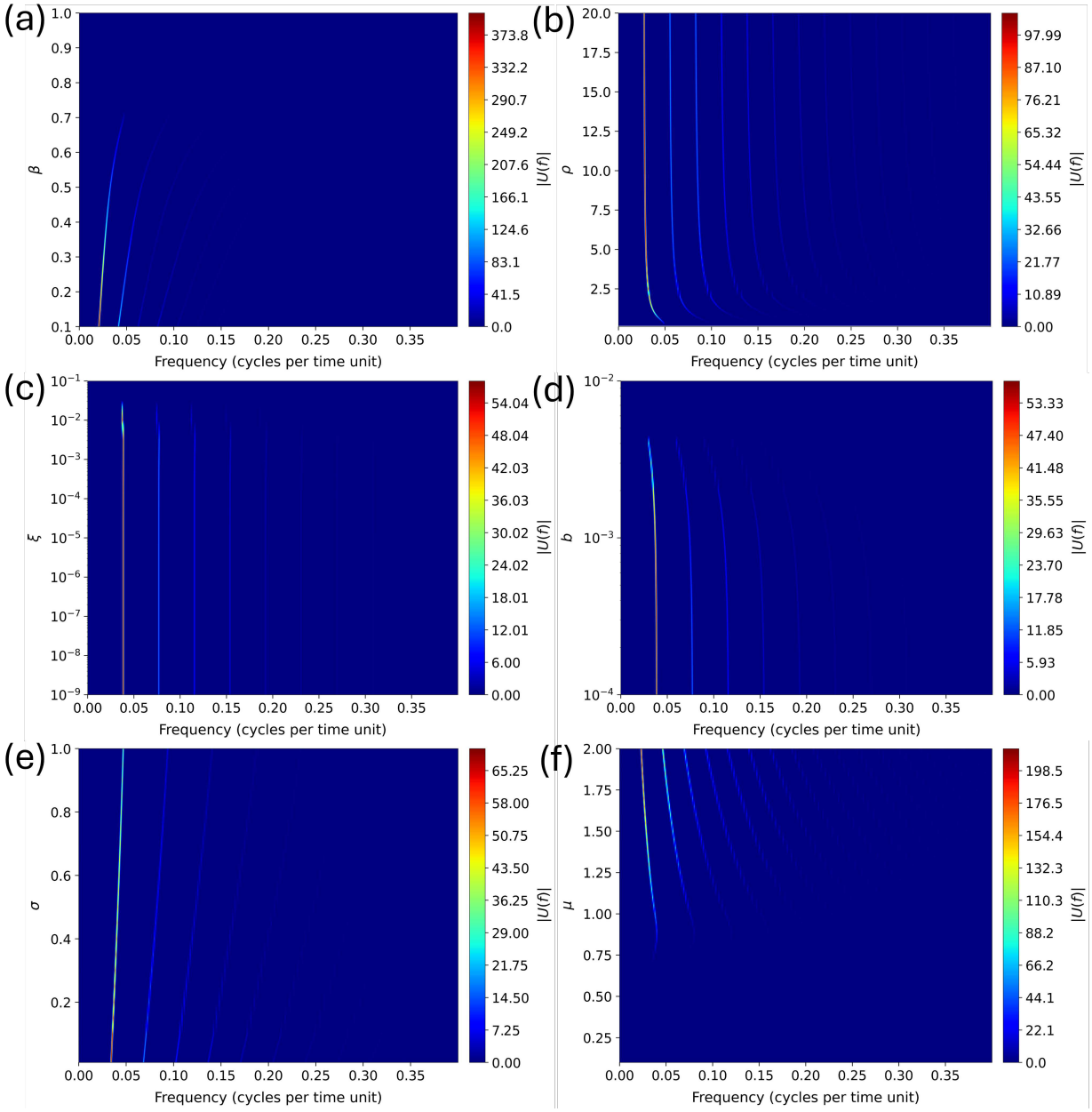


Figure 2: Fourier magnitude $|U(f)|$ of the tumor population under one-parameter sweeps of (a) CTL-mediated tumor killing β, (b) CAR-T-mediated tumor killing ρ, (c) tumor-induced CTL deactivation ξ, (d) tumor-induced CAR-T deactivation b, (e) CAR-T-associated CTL loss σ, and (f) CTL-dependent CAR-T activation μ.

Figure 4(a)–(e) show how the steepness coefficients affect the frequency comb spacing. l_1, l_2, and l_4 increase the frequency combs spacing; l_3 decreases it; l_0 non-monotonously affect the frequency comb spacing. Also, the frequency combs are found to exist only for the fractional orders in the range $0.9 \lesssim \alpha \leq 1$.

4 Conclusion

What this model shows, in the end, is that tumor cells, CTLs, and CAR-T cells need nothing beyond their own autonomous interactions to produce a *biological frequency comb*. The three populations oscillate at the same time

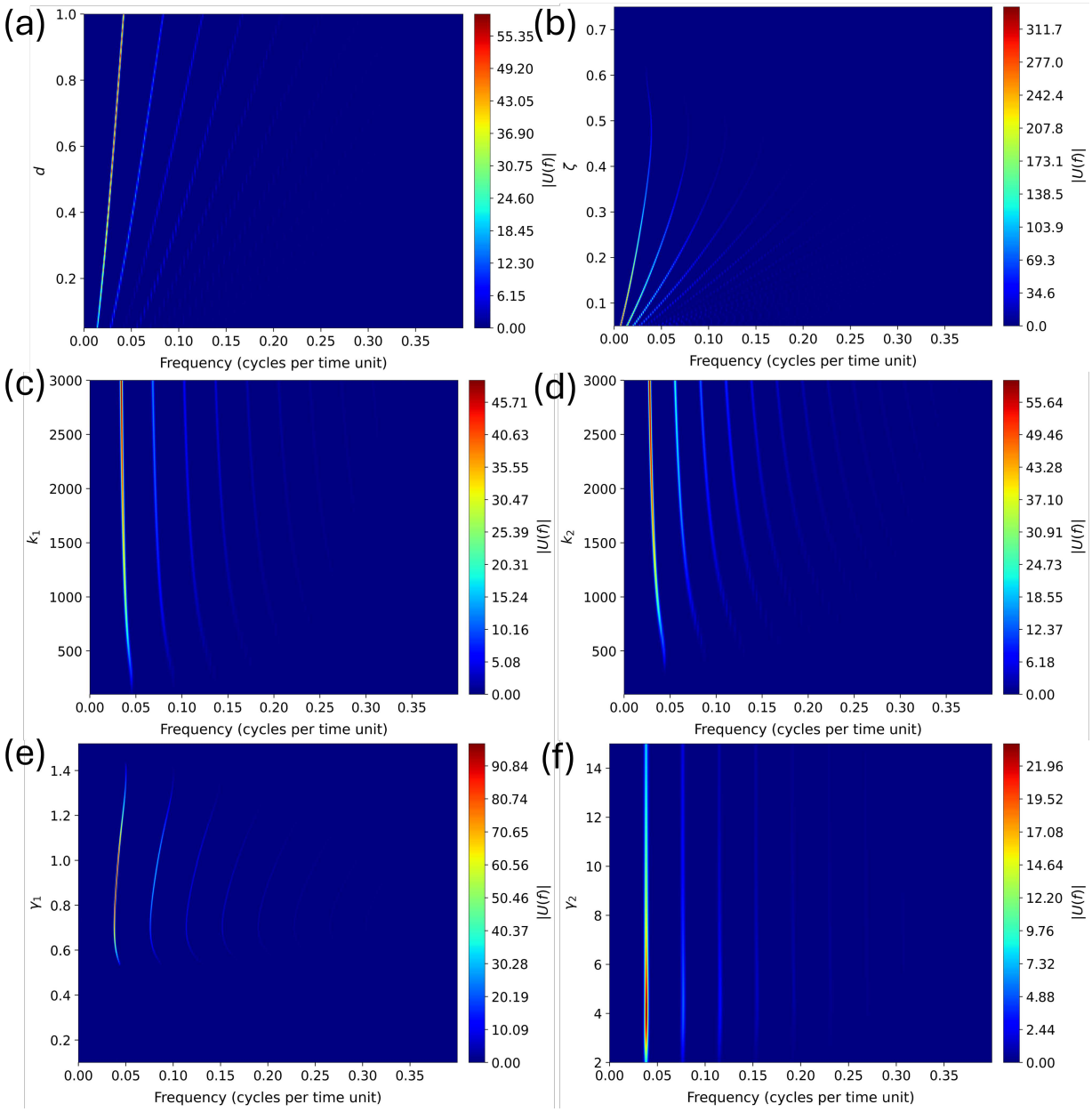


Figure 3: One-parameter sweeps of the Fourier magnitude $|U(f)|$ for (a) CTL decay d, (b) CAR-T decay ζ, (c) tumor carrying capacity k_1, (d) CTL carrying capacity k_2, (e) tumor growth rate γ_1, and (f) CTL growth rate γ_2.

period, with their oscillation spectra constituting one fundamental frequency and multiple harmonics. By lowering the CAR-T cell decay rate, the time period of the oscillations increases with the corresponding reduction in the fundamental frequency and the increase in the number of harmonics. In summary, β, σ, d, ζ, l_1, l_2, and l_4 increase the frequency comb spacing; b, μ, k_1, k_2, and l_3 decrease it; ξ and γ_2 have almost no influence; ρ, l_0 and γ_1 produce a nonmonotonous shift. Also, the frequency comb disappears at large enough values of β, b, or ζ, while μ and the carrying capacities (k_1 and k_2) should be set above a threshold value to produce a frequency comb. In the future, the experimental observation of these frequency comb oscillations and their use as non-invasive biomarkers for breast cancer can be demonstrated. Also, the idea of biological frequency combs can be extended to other diseases and biological systems.

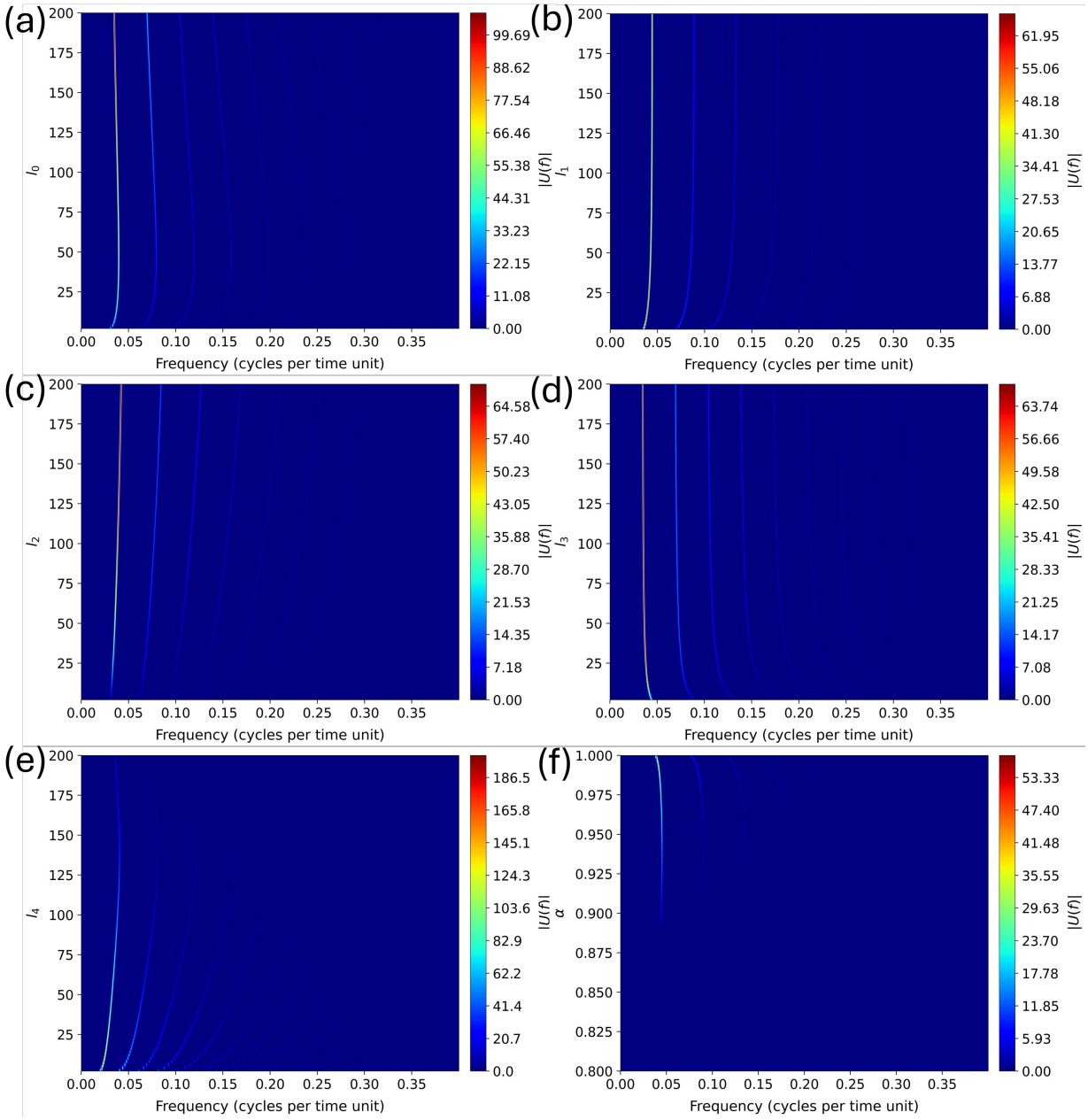


Figure 4: Fourier magnitude $|U(f)|$ under one-parameter sweeps of the steepness coefficients associated with (a) CTL-mediated tumor killing l_0, (b) CAR-T-mediated tumor killing l_1, (c) tumor-induced CTL proliferation l_2, (d) CTL-to-CAR-T-cell conversion l_3, and (e) CTL-mediated CAR-T-cell activation l_4, together with (f) the Caputo order α.

References

[1] Alan L. Hodgkin and Andrew F. Huxley. A quantitative description of membrane current and its application to conduction and excitation in nerve. *The Journal of Physiology*, 117(4):500–544, 1952. doi:10.1113/jphysiol.1952.sp004764.

[2] Alan M. Turing. The chemical basis of morphogenesis. *Philosophical Transactions of the Royal Society of London. Series B, Biological Sciences*, 237(641):37–72, 1952. doi:10.1098/rstb.1952.0012.

[3] Robert M. May. Simple mathematical models with very complicated dynamics. *Nature*, 261(5560):459–467, 1976. doi:10.1038/261459a0.

[4] John J. Tyson, Katherine C. Chen, and Bela Novak. Sniffers, buzzers, toggles and blinkers: Dynamics of regulatory and signaling pathways in the cell. *Current Opinion in Cell Biology*, 15(2):221–231, 2003. doi:10.1016/S0955-0674(03)00017-6.

[5] Albert Goldbeter. Computational approaches to cellular rhythms. *Nature*, 420(6912):238–245, 2002. doi:10.1038/nature01259.

[6] Bela Novak and John J. Tyson. Design principles of biochemical oscillators. *Nature Reviews Molecular Cell Biology*, 9(12):981–991, 2008. doi:10.1038/nrm2530.

[7] Boris N. Kholodenko. Cell-signalling dynamics in time and space. *Nature Reviews Molecular Cell Biology*, 7(3): 165–176, 2006. doi:10.1038/nrm1838.

[8] Geneviève Dupont, Laurent Combettes, Gary S. Bird, and James W. Putney. Calcium oscillations. *Cold Spring Harbor Perspectives in Biology*, 3(3):a004226, 2011. doi:10.1101/cshperspect.a004226.

[9] John J. Tyson and Bela Novak. Regulation of the eukaryotic cell cycle: Molecular antagonism, hysteresis, and irreversible transitions. *Journal of Theoretical Biology*, 210(2):249–263, 2001. doi:10.1006/jtbi.2001.2293.

[10] Galit Lahav, N. Rosenfeld, A. Sigal, N. Geva-Zatorsky, Arnold J. Levine, Michael B. Elowitz, and Uri Alon. Dynamics of the p53-Mdm2 feedback loop in individual cells. *Nature Genetics*, 36(2):147–150, 2004. doi:10.1038/ng1293.

[11] David E. Nelson et al. Oscillations in NF-κB signaling control the dynamics of gene expression. *Science*, 306 (5696):704–708, 2004. doi:10.1126/science.1099962.

[12] Michael B. Elowitz and Stanislas Leibler. A synthetic oscillatory network of transcriptional regulators. *Nature*, 403(6767):335–338, 2000. doi:10.1038/35002125.

[13] Tony Yu-Chen Tsai, Yoon Sup Choi, Wenzhe Ma, Joseph R. Pomerening, Chao Tang, and James E. Ferrell. Robust, tunable biological oscillations from interlinked positive and negative feedback loops. *Science*, 321(5885): 126–129, 2008. doi:10.1126/science.1156951.

[14] Jeremy E. Purvis and Galit Lahav. Encoding and decoding cellular information through signaling dynamics. *Cell*, 152(5):945–956, 2013. doi:10.1016/j.cell.2013.02.002.

[15] Joe H. Levine, Yihan Lin, and Michael B. Elowitz. Functional roles of pulsing in genetic circuits. *Science*, 342 (6163):1193–1200, 2013. doi:10.1126/science.1239999.

[16] Candela L. Szischik, Juliana Reves Szemere, Rocío Balderrama, Constanza Sánchez de la Vega, and Alejandra C. Ventura. Transient frequency preference responses in cell signaling systems. *npj Systems Biology and Applications*, 10(1):86, 2024. doi:10.1038/s41540-024-00413-w.

[17] Peng Zhao, Jian Liu, Tengfei Bao, Hong Huo, Ye Yuan, and Tao Fang. Flexible modulation of hybrid feedback loops in competitive biological oscillators. *npj Systems Biology and Applications*, 11(1):122, 2025. doi:10.1038/s41540-025-00594-y.

[18] Subhas Khajanchi and Juan J. Nieto. Mathematical modeling of tumor-immune competitive system, considering the role of time delay. *Applied Mathematics and Computation*, 340:180–205, 2019. doi:10.1016/j.amc.2018.08.018.

[19] Grace E. Mahlbacher, Kevin C. Reihmer, and Hermann B. Frieboes. Mathematical modeling of tumor-immune cell interactions. *Journal of Theoretical Biology*, 469:47–60, 2019. doi:10.1016/j.jtbi.2019.03.002.

[20] Chenhui Ma and Evren Gurkan-Cavusoglu. A comprehensive review of computational cell cycle models in guiding cancer treatment strategies. *npj Systems Biology and Applications*, 10(1):71, 2024. doi:10.1038/s41540-024-00397-7.

[21] Constantinos Harkos, Andreas G. Hadjigeorgiou, Chrysovalantis Voutouri, Ashwin S. Kumar, Triantafyllos Stylianopoulos, and Rakesh K. Jain. Using mathematical modelling and AI to improve delivery and efficacy of therapies in cancer. *Nature Reviews Cancer*, 25(5):324–340, 2025. doi:10.1038/s41568-025-00796-w.

[22] Thomas Udem, Ronald Holzwarth, and Theodor W. Hänsch. Optical frequency metrology. *Nature*, 416(6877): 233–237, 2002. doi:10.1038/416233a.

[23] Steven T. Cundiff and Jun Ye. Colloquium: Femtosecond optical frequency combs. *Reviews of Modern Physics*, 75(1):325–342, 2003. doi:10.1103/RevModPhys.75.325.

[24] Adarsh Ganesan, Cuong Do, and Ashwin Seshia. Phononic frequency comb via intrinsic three-wave mixing. *Physical Review Letters*, 118(3):033903, 2017. doi:10.1103/PhysRevLett.118.033903.

[25] Adarsh Ganesan, Cuong Do, and Ashwin Seshia. Phononic frequency comb via three-mode parametric resonance. *Applied Physics Letters*, 112(2):021906, 2018. doi:10.1063/1.5003133.

[26] Adarsh Ganesan, Cuong Do, and Ashwin Seshia. Excitation of coupled phononic frequency combs via two-mode parametric three-wave mixing. *Physical Review B*, 97(1):014302, 2018. doi:10.1103/PhysRevB.97.014302.

[27] Ata Keşkekler, Hadi Arjmandi-Tash, Peter G. Steeneken, and Farbod Alijani. Symmetry-breaking-induced frequency combs in graphene resonators. *Nano Letters*, 22(15):6048–6054, 2022. doi:10.1021/acs.nanolett.2c00360.

[28] Ian Anderson, Jack Kramer, Tzu-Hsuan Hsu, Yinan Wang, Vakhtang Chulukhadze, and Ruochen Lu. Phononic combs in lithium niobate acoustic resonators. *Applied Physics Letters*, 128(5):052201, 2026. doi:10.1063/5.0304587.

[29] Matthijs H. J. de Jong, Adarsh Ganesan, Andrea Cupertino, Simon Gröblacher, and Richard A. Norte. Mechanical overtone frequency combs. *Nature Communications*, 14(1):1458, 2023. doi:10.1038/s41467-023-36953-8.

[30] Guangzong Xiao, Zijian Feng, Tengfang Kuang, Ran Huang, Yutong He, Xinlin Chen, Yunlan Zuo, Xiang Han, Wei Xiong, Zhongqi Tan, Adarsh Ganesan, Franco Nori, Cheng-Wei Qiu, Xiaobao Zhang, Hui Luo, and Hui Jing. Ultrabroadband phonon laser frequency comb. *Advanced Photonics*, 8(2):026004, 2026. doi:10.1117/1.AP.8.2.026004.

[31] Hongbin Lei, Qian Zhang, Hongqiang Xie, Congsen Meng, Zhaoyang Peng, Xiaowei Wang, Jinlei Liu, Guangru Bai, Adarsh Ganesan, and Zengxiu Zhao. On the nonlinear rovibrational excitation of phononic frequency combs in molecules. *Optics Express*, 33(3):5396–5410, 2025. doi:10.1364/OE.544325.

[32] Rumeng Liu and Guangfei Zhu. Phononic frequency combs in twisted bilayer van der waals material resonators. *Journal of Applied Physics*, 138(14):144305, 2025. doi:10.1063/5.0296669.

[33] Murtaza Rangwala and Adarsh Ganesan. Spontaneous symmetry breaking and collective higgs-goldstone dynamics in solid-state phononic frequency combs. *arXiv preprint arXiv:2602.07462*, 2026.

[34] Shreyas Muralidhar, Ahmad A. Awad, A. Alemán, Roman Khymyn, Mykola Dvornik, Dag Hanstorp, and Johan Åkerman. Sustained coherent spin wave emission using frequency combs. *Physical Review B*, 101(22):224423, 2020. doi:10.1103/PhysRevB.101.224423.

[35] Xiyin Ye and Tao Yu. Frequency comb of electric-polarization waves, 2026. URL `https://arxiv.org/abs/2603.27947`.

[36] Oem Trivedi, Madhurendra Mishra, and Adarsh Ganesan. Cosmological frequency combs. *EPL (Europhysics Letters)*, 154(3):39001, 2026. doi:10.1209/0295-5075/ae55c4.

[37] Madhurendra Mishra, Oem Trivedi, and Adarsh Ganesan. Nonlinear dynamical regimes of cosmological frequency combs. *arXiv preprint arXiv:2606.16227*, 2026.

[38] E. Ahmed, A. H. Hashis, and F. A. Rihan. On fractional order cancer model. *Journal of Fractional Calculus and Applications*, 3(2):1–6, 2012. URL `https://journals.ekb.eg/article_283762.html`.

[39] Chandrali Baishya, R. N. Premakumari, J. R. Asharani, and Ebenezer Bonyah. Modeling breast cancer dynamics with fractional derivatives: Immunotherapy and circuit-based analysis. *Scientific African*, 29:e02842, 2025. doi:10.1016/j.sciaf.2025.e02842.